Alternating Block Copolymers Consisting of Oligo(phenylene) and Oligo(ethylene glycol) Units of Defined Length: Synthesis, Thermal Characterization, and Light-Emitting Properties

Matthew T. Hargadon,[†] Evan A. Davey,[‡] Tia B. McIntyre,[‡] Dinakar Gnanamgari,[‡] Cherise M. Wynne,[‡] Robert C. Swift,[‡] Jennifer R. Zimbalist,[‡] Brittany L. Fredericks,[‡] Anthony J. Nicastro,[†] and Felix E. Goodson*[,‡]

Departments of Chemistry and Physics, West Chester University of Pennsylvania, West Chester, Pennsylvania 19383

Received April 3, 2007; Revised Manuscript Received November 29, 2007

ABSTRACT: Polymers containing conjugated oligo(phenylene) segments of defined length alternating with solubilizing regions of di- to hexa(ethylene glycol) have been synthesized using a Suzuki coupling protocol. Soluble and characterizable materials with up to four benzene rings linked together have been formed without the inclusion of conjugation-disrupting solubilizing side chains. The polymers were generated with weight-averaged molecular weights as high as 158 000 g/mol as determined by GPC−LS. The thermal and luminescence properties of these materials were studied in order to determine how these properties varied with the lengths of the two types of blocks. While the terphenyl polymers were amorphous, the quaterphenyl polymers exhibited multiple transitions in their DSC thermatograms. Polarized light microscopy and X-ray diffractometry were used to investigate this behavior. All of the polymers fluoresced strongly in the blue region of the visible spectrum with a 40 nm red shift in emission between solution and solid-state spectra. UV−visible and fluorescence studies were performed at different concentrations and in solvent/nonsolvent mixtures in order to study possible causes for this spectral shift, which appears to be due to the presence of ground state aggregates.

Introduction

Since the discovery that poly(*p*-phenylene) conducts electricity when doped with oxidizing or reducing agents,[1] a great deal of research has gone into the study of this material and its derivatives.[2−8] Other interesting and important properties that poly(phenylene)s exhibit include liquid crystallinity[9] and photo- and electroluminescence.[10] Unfortunately, the rigid conjugated backbone largely responsible for these properties also renders underivatized poly(*p*-phenylene) insoluble and infusible. Consequently, it cannot be processed, and straightforward syntheses result in only oligomeric materials.[11] One strategy used to combat this problem has been to stitch solubilizing side chains onto the polymer backbone.[12] However, this can disrupt the conjugation and alter the sought-after properties.[13] Another approach is to incorporate flexible solubilizing groups in between blocks of the rigid, conjugated material.[14−19] This alternating rigid−flexible block copolymer strategy is well-established in the synthesis of main-chain liquid crystalline polyesters[20,21] and classic poly(urethane)-based thermoplastic elastomeric materials.[22]

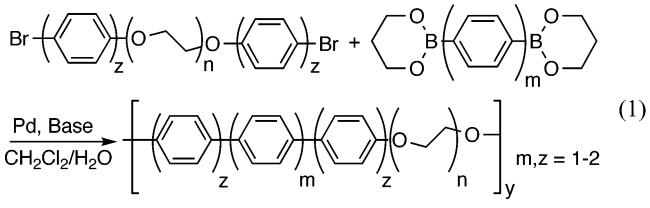

(1)

Previously, we reported on the synthesis of alternating rigid−flexible block copolymers which incorporated oligo(phenylene) units of defined length in the rigid blocks (eq 1, $n_{avg} = 23$).[23] The flexible poly(ethylene glycol) units provided solubility and processability without disrupting the conjugation of the oligo(phenylene) blocks. Unfortunately, the molecular weights were not as high as we had hoped (maximum $M_n = 19\,600$). This could prove to be problematic if these materials were to be used in LEDs or other potential applications since the materials properties of a polymer are strongly dependent upon its molecular size. These insufficient molecular weights were most likely due to a small amount of contamination of the dibromide macromonomers with monofunctional chains caused by incomplete reactions during the monomer synthesis.[23] Since these monomers were nonvolatile oils, we were unable to purify them effectively from the monofunctional contaminants.

An obvious solution to this problem would be to synthesize polymers with oligo(ethylene glycol) spacers (eq 1, $n = 1-6$).[24−26] The smaller size should make the monomers easier to purify through standard distillation and possibly recrystallization methods. Unfortunately, our attempts here with all *para*-linked phenyl rings did not result in soluble materials. However, we more recently discovered that when the flexible block is linked to the polyphenylene block in the *meta* rather than *para* positions, soluble polymers with as few as two ethylene glycol units in the flexible block could be formed (eq 2) with high molecular weights. In this paper, we present studies on the synthesis, characterization, thermal properties, and light-emitting capabilities of these materials.

Results and Discussion

The dibromide monomers (**1**−**6**) were conveniently synthesized from the corresponding ditosylates under standard Will-

* To whom correspondence should be addressed. E-mail: fgoodson@wcupa.edu.
[†] Department of Physics, West Chester University of Pennsylvania.
[‡] Department of Chemistry, West Chester University of Pennsylvania.

10.1021/ma070796n CCC: $40.75
Published on Web 01/16/2008

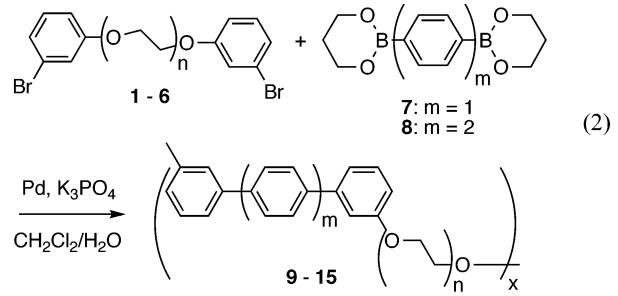

(2)

iamson Ether Synthesis conditions (eq 3). Analytically pure samples were obtained in moderate to good yields (60−72%) upon column chromatography of the crude products followed by recrystallization and/or kugelrohr distillation. Unlike the case for the macromonomers synthesized from poly(ethylene glycol),[23] there was no indication of hydroxyl end caps visible by ^{13}C NMR.[27]

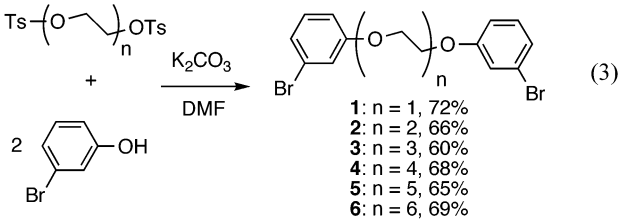

(3)

Polymers **9**−**15** were then obtained via a Suzuki coupling[28−30] polycondensation[2,6] under optimized conditions[31] of **1**−**6** with the appropriate diboronic ester monomers **7** and **8** (eq 2, Table 1). As can be seen from these data, polymers were isolated in moderate to good yields with molecular weights significantly higher than polymers obtained with the macromonomer strategy.[23] Indeed, the molecular weight for polymer **15** in particular is quite high when compared with other light-emitting polymers synthesized via a Suzuki polycondensation.[32−35]

Interestingly, attempts at forming the polymer with three ethylene glycol units in the flexible block led only to insoluble materials, even though polymer **9**, with a shorter spacer, was freely soluble in chloroform. While we first believed that this might be due to this polymer being formed with a particularly high molecular weight, the fact that chloroform-soluble fractions contained only oligomeric material suggests that even moderately sized chains do not dissolve, and that this insolubility is an inherent property of the material.

The molecular weights were measured via tandem GPC−MALS (gel permeation chromatography−multiangle light scattering), a technique that also required the determination of the refractive index increment of these materials (Table 1). While these values may seem anomalously large at first glance, conjugated polymers are known to exhibit exceptionally high refractive index increments in comparison with nonconjugated materials.[36] Also of note is the fact that the quaterphenyl copolymers (**11**, **13**, **15**) exhibit higher values than the corresponding terphenyl materials with similar phenylene weight percent (Figure 1). This is likely caused by the increased conjugation provided by the longer oligo(phenylene) blocks in the former series of polymers, in agreement with trends seen with *p*-phenylene oligomers.[37]

Figure 2 shows typical GPC chromatograms for polymer **15**. The low molecular weight peaks are most likely caused by contamination with a small amount of cyclic oligomer, the formation of which is unfortunately facilitated by the *meta* regiochemistry of the monomers.[38] However, as the chromatograms show, these impurities were readily removed by a Soxhlet extraction with ligroin for the polymers with three phenyl rings (**9**, **10**, **12**, **14**), or toluene for the polymers with four (**11**, **13**, **15**). (The particularly narrow polydispersities for the more soluble materials were probably a result of the toluene/ligroin extractions rinsing away some lower molecular weight linear chains along with the intended cyclic oligomers.)

Figure 3 presents ^{1}H and ^{13}C NMR spectra for polymer **13**. The signals due to the internal *para*-substituted benzene rings converge into a narrow AA′BB′ pattern at 7.7 ppm, while the external rings exhibit typical *meta*-substitution resonances between 6.8 and 7.5. Similarly, the ^{13}C spectrum shows the

Table 1. Polymerization Results

monomers	polymer	*m*	*n*	% yield	d*n*/d*c*[a]	% *P*[b]	M_n[c]	M_w[d]
1 + **7**		1	1	*e*	*e*	*e*	*e*	*e*
2 + **7**	**9**	1	2	81	0.198	69	27 500	56 600
2 + **8**		2	2	*e*	*e*	*e*	*e*	*e*
3 + **7**		1	3	*e*	*e*	*e*	*e*	*e*
4 + **7**	**10**	1	4	74	0.167	54	26 800	52 700
4 + **8**	**11**	2	4	54[f]	0.198	61	68 000[f]	122 000[f]
5 + **7**	**12**	1	5	90	0.155	49	40 800	88 400
5 + **8**	**13**	2	5	81	0.184	56	21 200	46 000
6 + **7**	**14**	1	6	54[g]	0.144	45	60 600[g]	78 100[g]
6 + **8**	**15**	2	6	58[g]	0.170	52	89 400[g]	158 000[g]

[a] Refractive index increment (in mL/g) measured at 690 nm and 25.0 °C in chloroform. [b] Weight percent from the phenylene block. [c] Number-averaged molecular weight (in g/mol) measured by tandem GPC−MALS. [d] Weight-averaged molecular weight (in g/mol) measured by tandem GPC−MALS. [e] Material was found to be insoluble in common solvents (including chloroform). Further attempts at purification and characterization were not performed. [f] Data reflect chloroform-soluble fractions only. [g] Low molecular weight fractions were lost in the purification, resulting in lower yields and narrower polydispersities.

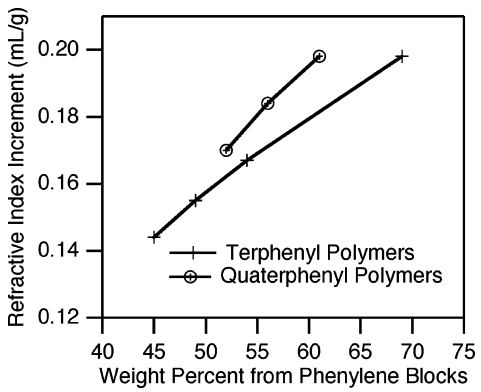

Figure 1. Refractive index increments for polymers **9**−**15** as a function of their weight percent from the conjugated phenylene regions.

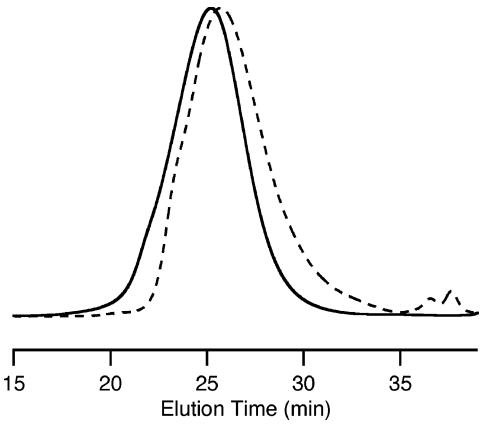

Figure 2. GPC chromatograms for polymer **15** before (dashed line) and after (solid line) a Soxhlet extraction with toluene.

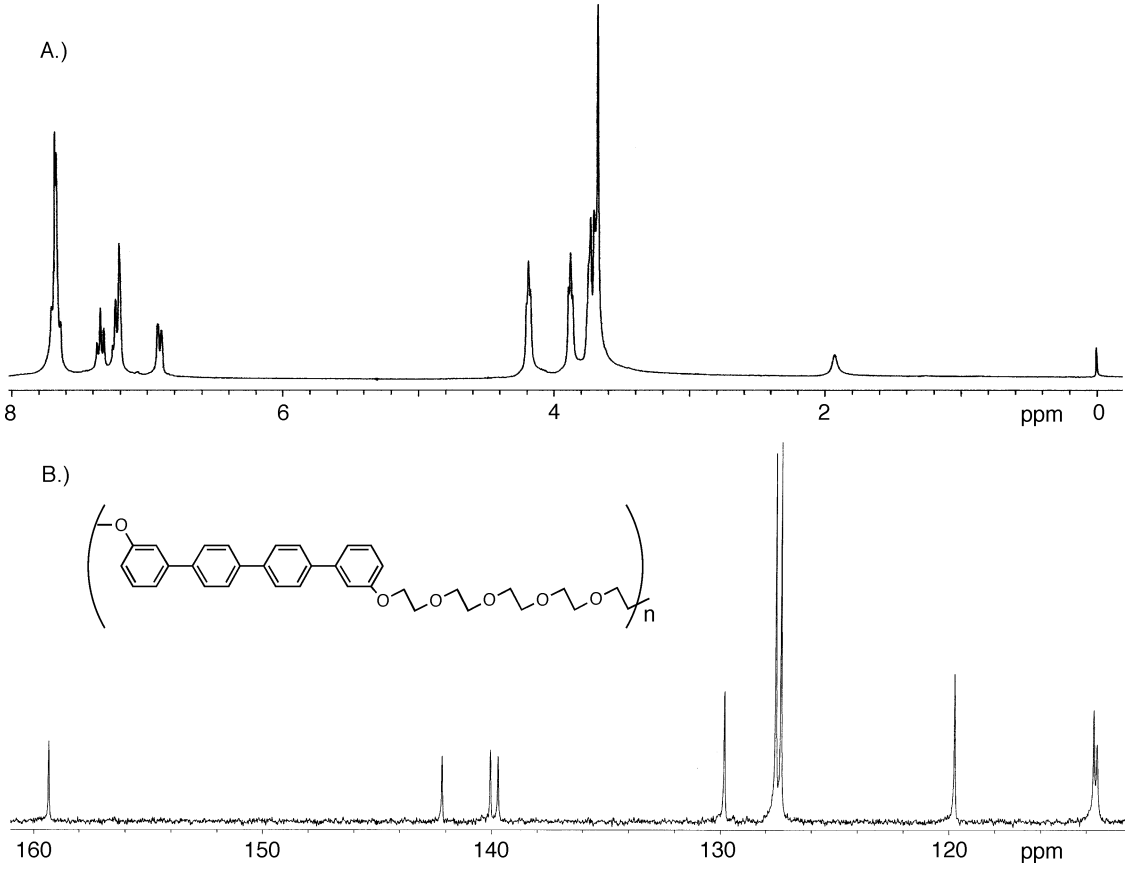

Figure 3. (A) ^{1}H and (B) ^{13}C (aromatic region) NMR spectra for polymer **13**.

Table 2. Thermal Properties of Polymers

polymer	*m*	*n*	T_d (°C)[a]	T_g (°C)[b,c]	*T* (°C)[b,d]
9	1	2	455	78	*e*
10	1	4	440	33	*e*
11	2	4	435	60	135(0.7), 142(−0.6), 177(11.0),[f] 179(−7.1),[f] 189(10.5)[f]
12	1	5	435	17	*e*
13	2	5	430	47	106(0.5), 119(−0.4), 147(18.3),[f] 149(−3.5),[f] 156(12.0)[f]
14	1	6	430	8	*e*
15	2	6	430	27	96(2.3), 105(−6.1), 123(13.0)

[a] Onset temperature for decomposition, as measured by TGA under nitrogen. [b] Measured by DSC (10 °C/min) during second heating cycle (See Figure 4). [c] Glass transitions determined from the midpoint of the transition step in the heating curve. [d] Additional thermal transitions (integrations in J/g), temperatures measured at peak maximum. [e] No additional transitions observed via DSC. [f] Determined at 1 °C/min.

expected ten signals in the aromatic region between 110 and 160 ppm. The lack of other resonances in this region indicates regular regiochemistry repeated throughout the polymer chain, as expected for a material generated by a Suzuki coupling polycondensation.

Analyses by TGA (under nitrogen) indicate that these materials are thermally stable up to >400 °C (Table 2). Decomposition occurs cleanly and sharply between 430 and 460 °C to yield between 5 and 15% char. The materials also show interesting behavior in their DSC traces (Table 2). The polymers with three phenyl rings (**9**, **10**, **12**, **14**, Figure 4A) show clear glass transitions, but no melting events, indicating that they are almost completely amorphous with very little if any crystallinity. (A slight amount of crystallinity is evident for polymer **9** when observed via polarized light microscopy, but not for the other terphenyl polymers.) Not surprisingly, the T_g decreases with increasing length of the oligo(ethylene glycol) spacer, in accordance with the thermal behavior of similar alternating block copolymers.[24−26]

Interestingly, the addition of a single phenyl ring in the rigid block has a more profound effect on polymer morphology. Polymers **11**, **13**, and **15**, with four phenyl rings (Figure 4B), exhibit only subtle glass transitions (which are approximately 30° higher than those for the terphenyl polymers) and multiple higher temperature thermal phenomena. In particular, polymer **15** showed a clear endotherm at 96 °C, followed immediately by an exothermic peak at 105 °C, and ultimately by a second endothermic transition at 123 °C. For polymers **11** and **13**, the first endotherm and exotherm are much less pronounced, and occur, not unexpectedly, at higher temperatures. More interestingly, the final endotherm is split into two distinct transitions for these two polymers. When the temperature was ramped downward, all three materials exhibited pronounced supercooling for the corresponding crystallization phenomena, with a strong dependence upon ramping rate (Figure 5), a characteristic typical of first-order transitions with relatively large discontinuities in order. For **11** and **13**, the crystallization events corresponding to the two melting transitions converge into a single peak; while, for **15** two exothermic transitions are evident. At very slow heating rates (1 °C/min), an exothermic peak between the two endotherms becomes apparent for polymers **11** and **13**; while a second crystallization event appears at extremely rapid cooling rates for **13** (although not for **11**). (The other polymers did not exhibit new features in their DSC traces upon slow heating or rapid cooling).

We next investigated the thermal behavior of polymers **11**, **13** and **15** via polarized light microscopy (PLM). Samples were prepared in the melt between a glass slide and a coverslip, and quickly cooled to room temperature. The microscopy of polymer **15** proved to be unremarkable. At room temperature, its

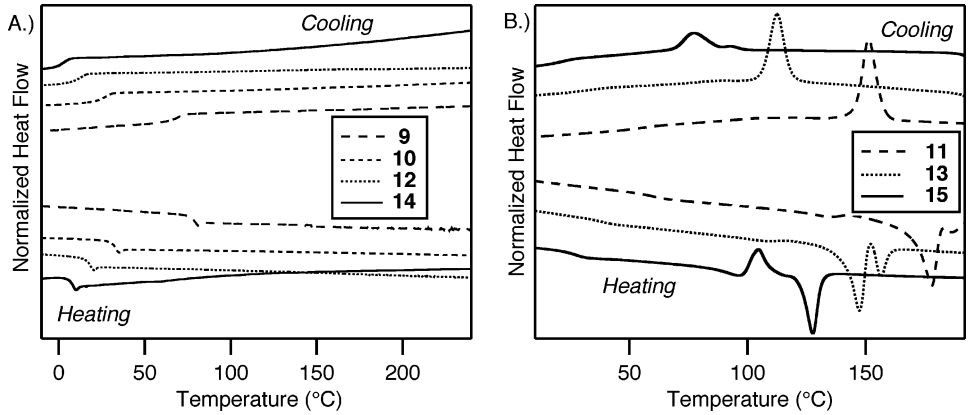

Figure 4. DSC thermatograms normalized to the same sample mass (first cooling cycle, second heating cycle, 10 °C/min) for (A) terphenyl and (B) quaterphenyl polymers. Exothermic peaks point up.

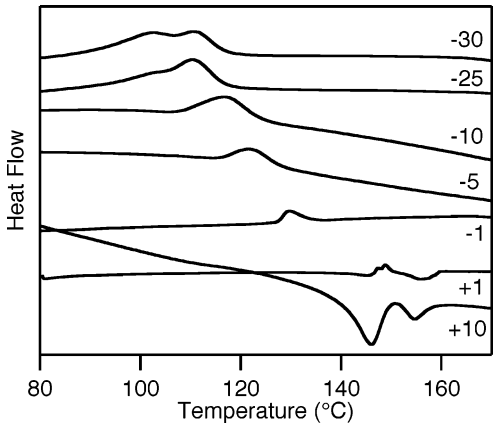

Figure 5. DSC thermatograms (multiple cycles) for polymer **13** (0.932 mg sample size) at different heating and cooling rates (in °C/min). Exothermic peaks point up.

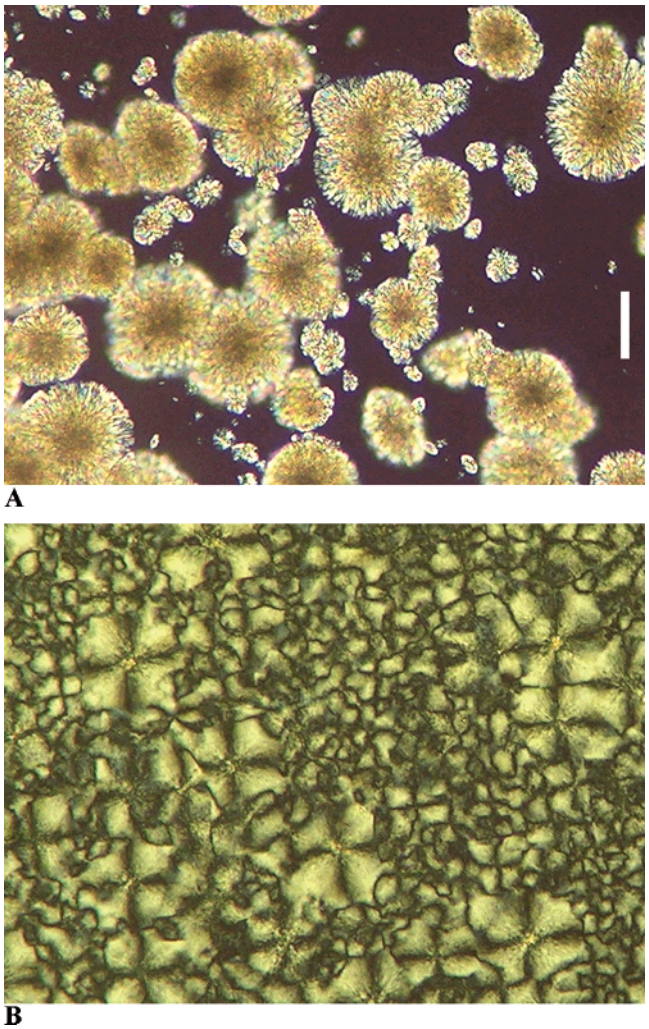

Figure 6. Polarized light microscopy of polymer **11** (A) at 169 °C, cooling from the melt at 1 °C/min, and (B) at 189 °C upon heating at 1 °C/min (second cycle). The white bar in part A represents 50 μm for both pictures.

microcrystalline nature exhibited itself as a granular texture that encompassed the entire field of view. This texture remained unchanged as the sample was heated (10 °C/min) until the birefringence disappeared at the polymer's melting point. The fact that there were no noticeable changes at the temperatures for the first transitions observed via DSC suggests that these events are due to a rearranging and crystallization of some of the amorphous regions of the polymer sample. The same texture reappeared uneventfully upon cooling at the same rate. Polymers **11** and **13** behaved similarly, except that upon cooling (1 or 10 °C/min) from the melt, they formed much larger crystallites that agglomerated into colorful spherulites (Figure 6A). Upon reheating (1 °C/min), there was no noticeable change at the temperature of the first endotherm (177 °C for **11**, 147 °C for **13**). At the higher temperature peak, the texture faded and sharpened to give defined Maltese cross patterns (Figure 6B), indicative of uniaxial ordering, immediately prior to isotropization.

The multiple thermal transitions observed by DSC, as well as the different textures evident from PLM, led us to speculate that polymers **11** and **13** may exhibit polymorphism and perhaps liquid crystallinity. To investigate this possibility we next studied the thermal behavior of these materials via X-ray diffraction (Figure 7). Polymers **11**, **13**, and **15** all exhibited the same basic pattern, indicating that they exist in the same crystalline morphology, despite the different behavior observed via DSC and PLM (there was no apparent correlation between the *d*-spacing of the peaks and the length of the flexible blocks). This pattern was completely independent of thermal history. In particular, samples of **13** that were quenched from the melt, annealed at 148 °C (between the two DSC endotherms) for 30 min, or cooled slowly (1 °C/min) from the melt, all yielded the same basic diffractogram, an observation that argues against the possibility of polymorphism.[39] Upon heating at 1 °C/min (between acquisitions), the diffraction patterns for **11** and **13** shifted (toward larger *d*-spacing) and broadened, until they had completely disappeared by the temperature of the lower-temperature DSC endotherm (even though no indication of

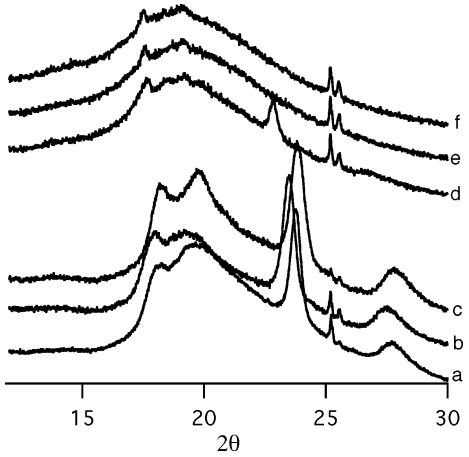

Figure 7. X-ray diffraction powder patterns (normalized to maximum intensity) for (a) **11**, (b) **13**, and (c) **15** at room temperature as well as for **13** at (d) 140 °C, (e) 147 °C, and (f) 165 °C. The two peaks at $2\theta = 25.2$ and 25.5° are due to the ceramic sample holder.

melting was observed via PLM until the high-temperature event). Upon cooling (1 °C/min), polymer **13** exhibited the same pattern, with the first indications of peaks becoming evident at 127 °C.

This loss of the Bragg patterns (at temperatures where the samples remain birefringent by PLM) would be consistent with a sample losing long-range order while maintaining short-range interactions, such as would the be case for the formation of a liquid crystalline phase. However, the fact that there were no changes in the textures observed via PLM at these temperatures argues against the occurrence of a phase transition. Furthermore, since isotropic to liquid crystal transformations (upon cooling) typically occur with very little supercooling, and with weak dependence of undercooling on the temperature ramp rate,[40,41] the DSC observations mentioned above also seem to indicate that a liquid crystalline phase is unlikely. Another explanation is that the two endotherms upon heating may reflect melting in the bulk (observed via X-ray) vs melting at the surfaces (observed via microscopy). Alternatively, the low-temperature event may be due to a softening of the ethylene glycol regions (resulting in the loss of long-range order), while the higher temperature transition may be caused by the melting of the oligophenylene regions (resulting in the loss of birefringence). Others have had success at inducing liquid crystallinity in alternating rigid−flexible block copolymers by introducing asymmetry into the repeating structure (i.e., through the inclusion of a chiral center,[42] the synthesis of random copolymers with different flexible segments,[43] the incorporation of regioirregularity into the structure of either the rigid[44] or flexible[45] blocks, etc.) We are currently investigating the application of these strategies in order to impart liquid crystallinity in our polymers.

Also of interest are the light-emitting properties of these materials. A serious problem with emissive polymers is that they tend to form either excimers (dimers between an excited chromaphore and a ground state molecule) or ground state aggregates (which result from emitting species associating before excitation), both of which can exhibit significant red-shifts in their solid-state emission (relative to solution) with markedly reduced quantum efficiencies.[46−48] Alternating block copolymer architectures such as the one presented here have been proven to be an effective strategy in preventing excimer formation in other polymer systems.[49,50]

Absorption and emission fluorescence spectra for selected alternating rigid−flexible block copolymers are presented in Figure 8, along with the relevant data in Table 3. All of the polymers emit strongly in the blue region of the visible spectrum. Not surprisingly, the absorption and emission maxima shift to the red as length of the conjugated rigid block increases from three to four phenyl rings; while the size of the flexible block has little effect on the fluorescence spectra of the materials. The quantum efficiencies are generally close to those of the parent terphenyl and quaterphenyl compounds (58 and 62% respectively[51−53]), though there appears to be a slight downward trend with increasing length of the flexible block. This may be due to a corresponding increase in the percentage of oxygen atoms in the polymer chains since heteroatoms have been shown to quench luminescence in other systems.[54] Alternatively, the cause could be an increased likelihood of nearby fluorophores within the same chain to associate with the additional mobility provided by the longer ethylene glycol regions. Others have noted an increase in intrachain aggregation between fluorophores in a polymer with an increase in backbone flexibility.[55]

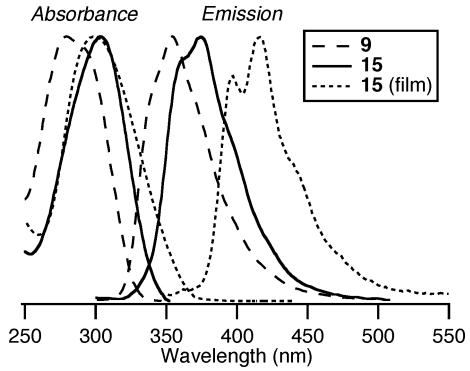

Figure 8. Absorbance and fluorescence spectra (normalized to maximum intensity) for $CHCl_3$ solutions of polymers **9**, and **15**, along with thin-film absorption and emission spectra for polymer **15**.

Table 3. Light-Emitting Properties of Polymers

polymer	*m*	*n*	λ_{max}(abs)[a]	λ_{max}(em)[b]	λ_{max}(film)[c]	Φ (%)[d]
9	1	2	279	354	385	59
10	1	4	279	355	386	56
11	2	4	304	375	418	60
12	1	5	280	354	388	58
13	2	5	304	375	415	57
14	1	6	280	354	389	54
15	2	6	303	375	416	53

[a] Wavelength (in nm) of maximum absorbance in the UV−vis spectrum. [b] Wavelength (in nm) of maximum fluorescence in the emission spectrum. Terphenyl polymers were excited at 280 nm, quaterphenyl polymers at 300 nm. [c] Wavelength (in nm) of maximum fluorescence in the emission spectrum of a solid polymer film on a quartz substrate. Terphenyl polymers were excited at 280 nm, quaterphenyl polymers at 305 nm. [d] Quantum yield based upon a terphenyl standard for polymers **9**, **10**, **12**, **14** and a quaterphenyl standard for polymers **11**, **13**, **15**.

Table 3 and Figure 8 also include data for absorption and emission spectra obtained on solid films. In all cases, the solid-state emission spectra are red-shifted by approximately 30−40 nm (still well within the blue) relative to those obtained in solution. Red shifts similar to those exhibited by our polymers have been attributed to excimers,[56] to pre-excitation association (caused by $\pi-\pi$[17,57] or hydrogen-bonding[58] interchromaphore interactions) and to an increased planarity of the conjugated segments in the solid-state relative to solution.[59] On the other hand, there is a slight blue shift in the solid state absorption spectra of the polymers.[60]

Others have investigated the tendency of a material to form ground state aggregates and/or excimers by studying its solution light-emitting behavior at different concentrations and in solvent/

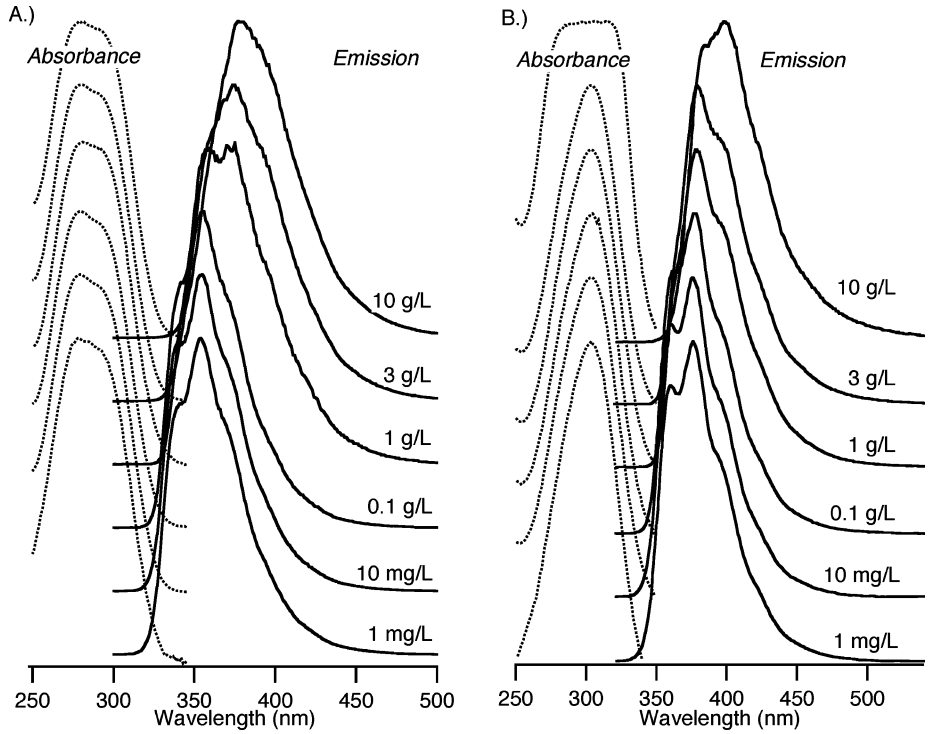

Figure 9. Absorbance and fluorescence spectra (normalized to maximum intensity) for $CHCl_3$ solutions of polymers **14** (A) and **15** (B) at different concentrations.

nonsolvent mixtures.[61,62] The absorption and emission spectra for polymers **14** and **15** at different concentrations in chloroform are presented in Figure 9. The emission spectra show no change until relatively high concentration (100 mg/L), at which point the high energy shoulders start to fade, and the main peaks shift toward the red. This trend continues with higher concentrations, with the longer wavelength shoulders becoming the major peaks at 10 g/L. The fact that the absorption spectra remain unchanged during this process suggests that this shift is due to the formation of excimers, rather than aggregates, since the former occur once photon absorption has already taken place.[61] Further evidence for this is provided by the fact that there was no change in the fluorescence spectra for the 3 g/L solutions before and after passing them through a 0.1-μm filter. (More concentrated solutions were too viscous to filter.) It is worth noting that the above red shift (and thereby excimer formation) occurs at much higher concentrations than for other systems that have been studied in this fashion.[61,62]

Figure 10 presents the absorption and emission spectra of chloroform solutions of **14** and **15** to which varying amounts of methanol (a nonsolvent) have been added. (All solutions maintained their optical clarity throughout this procedure.) As before, emission spectra shift toward the red with increasing methanol, with the spectrum at 65% methanol approaching that for the solid state. Ground state aggregates are typically characterized by additional absorption bands appearing upon their formation.[46,61,62] While there is no indication of any such bands in the spectra shown in Figure 10, there is a noticeable red-shift as the methanol content is increased to 65%, followed by a sudden and surprising blue shift at 80%. This type of abrupt hypsochromic shift with the addition of a poor solvent to a polymer solution has been noted before, and attributed to the formation of colloidal aggregates.[63] When the 65% methanol solutions are passed through a 0.1-μm filter, the overall fluorescence is quashed by 90%, an observation that further proves aggregation is occurring. Furthermore, the emission spectra of the filtrates are close to those of the original chloroform solutions, which indicate that the red-shifted emissions are due to these aggregates. As is the case with other systems,[47,48] this red shift is accompanied by a reduction in quantum efficiency (which for the 65% methanol solution of **15** is decreased to 23%). While it is tempting to suggest that the blue shift in the absorption spectra may be due to a transition in the mode of fluorescence quenching (from ground state aggregates to excimers), the fact that the 80% methanol spectra do not overlap with the chloroform spectra (the former are considerably broader), indicates that aggregates are still the cause of the red-shifted emission. More likely, the blue shift is due to a conformational change, resulting in an increase in the cant angle between adjacent phenyl rings, as the chains in the aggregates pack closer together in the poorer solvent. It is also worth noting that the absorption spectra of the solid films closely match those of the 80% methanol solutions. This, combined with the fact that these spectra do not overlap with those of the concentrated polymer solutions in Figure 9 (where excimers are occurring), suggests that the red shift in solid-state emission of these polymers is due to the presence of ground state aggregates, rather than excimers. Nevertheless, it should be emphasized that these emissions are still well within the blue region of the visible spectrum.

The light-emitting properties of these polymers may make them useful candidates for applications in electroluminescent and photovoltaic devices. Granted, it is unlikely that these materials will match the outstanding luminescence performance of the more established poly(fluorene) derivatives.[64−66] However, the relatively simple monomer synthesis (a single step from commercial precursors) for the polymers presented here and the high molecular weights (when compared with those of other light-emitting polymers in the literature), as well as the ease by which the thermal and morphological properties can be adjusted (by simply varying the length of the two blocks), should make them attractive alternatives for specific applications.

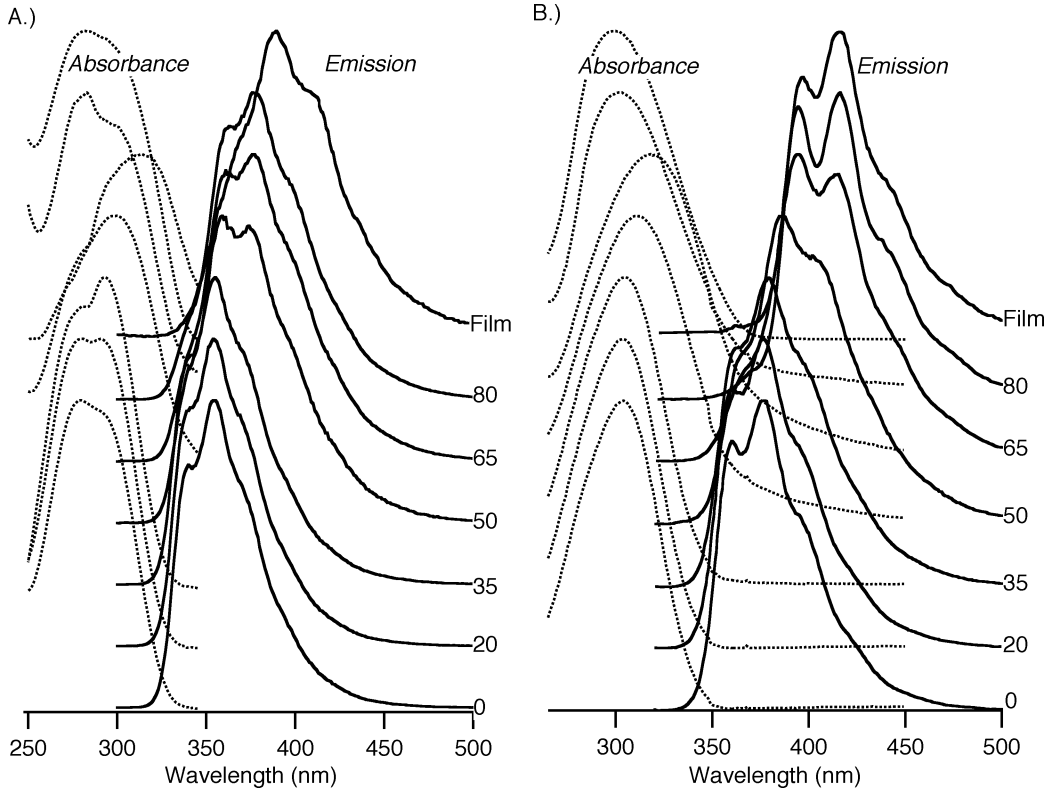

Figure 10. Absorbance and fluorescence spectra (normalized to maximum intensity) for $CHCl_3$/MeOH solutions (approximately 10 mg/L) of polymers **14** (A) and **15** (B). Numbers indicate percent methanol (v/v).

Conclusions

In summary, we have been able to synthesize alternating rigid−flexible block copolymers with defined lengths of conjugated oligo(phenylene) blocks and solubilizing oligo(ethylene glycol) spacers. Most of these polymers are freely soluble in chloroform, as long as the blocks are joined in the *meta* position of the terminal phenyl rings of the rigid blocks. Monomers incorporating the smaller oligo(ethylene glycol) spacers were considerably easier to purify than their macromonomer analogs, a fact that enabled us to isolate materials with significantly higher molecular weights (as high as $M_w = 158\,000$ g/mol).

The materials showed interesting thermal behavior. While polymers with three phenyl rings in their rigid blocks were amorphous, those with four were semicrystalline and exhibited multiple transitions in their DSC thermatograms. Finally, the materials all fluoresced strongly in the blue region of the visible spectrum. Evidence for aggregate formation was provided by absorption and fluorescence spectroscopy at different concentrations, and with the addition of varying amounts of methanol. While these associations did result in a 30−40 nm red shift in the emission of the polymers from the solution to the solid state, it was not enough to shift the visible color significantly.

Experimental Section

General Data. 3-Bromophenol was obtained from a commercial supplier and distilled through a vigreux column under vacuum prior to use. Hexaethylene glycol di(*p*-toluene)sulfonate was synthesized via a literature procedure.[67] Diboronic ester monomers, 1,4-bis-(1,3,2-dioxaborolan-2-yl)benzene (**7**), and 4,4′-bis(1,3,2-dioxaborolan-2-yl)biphenyl (**8**), were generated by esterifying the commercially available boronic acids with 1,3-propanediol as described in the literature,[23] and recrystallized several times from toluene (**7**) or benzene (**8**) until constant melting points (229 °C for **7**, 231 °C for **8**) were measured. All other chemicals were used as received from chemical suppliers. Nuclear magnetic resonance spectra were obtained at 300 MHz (proton) and 75 MHz (carbon) using a General Electric QE 300 NMR spectrometer, or at 400 MHz (proton) and 100 MHz (carbon) using a Bruker Avance-III 400 NMR spectrometer. Differential scanning calorimetry measurements were performed with a Mettler Toledo DSC821e instrument. A TA Instruments 2050 Thermogravimetric analyzer was used to obtain TGA data. Molecular weights were measured in chloroform solution with a tandem GPC−LS apparatus that consisted of an Agilent Technologies Series 1100 HPLC pump equipped with Waters Styrogel GPC columns (HR5E, HR4, HR4E connected in series) in line with a Wyatt Technologies DAWN-EOS light scattering photometer and a Wyatt Optilab DSP interferometric refractometer. Measurements were made at 25.0 °C and a wavelength of 690 nm. Refractive index increments were measured under the same conditions by injecting polymer solutions of known concentrations into the above refractometer with a syringe pump. Fluorescence spectra were obtained with a Cary Eclipse fluorescence spectrophotometer. UV−visible spectra were obtained with a Cary Bio 300 UV−visible spectrophotometer. Spectra for concentrated solutions were recorded using a 1 mm quartz cell and a 0.064 mm NaCl IR solution cell. Quantum yields were determined with chloroform solutions via the method of Fery-Forgues,[68] utilizing the above fluorimeter and spectrophotometer. For the polymers with three phenyl rings, *p*-terphenyl ($\Phi = 58\%$[51−53]) was used as a fluorescence standard, while *p*-quaterphenyl ($\Phi = 62\%$[51−53]) was utilized for the polymers with four. Solutions were degassed via three freeze−pump−thaw cycles, and samples were prepared in an argon-filled glovebox in order to eliminate the effects of oxygen quenching. Microscopic observations and measurements were conducted with a Zeiss Amplivol polarizing microscope equipped with an Instec HS1 hot stage and STC 200 temperature controller. In the temperature range in which the hot stage was operated, its accuracy was ±0.4 °C, but its temperature stability was approximately ±0.05 °C. Photographs were taken with a Nikon Coolpix 8700 digital camera equipped with an 8X zoom. X-ray diffraction data were obtained with a Paar Physica X"Pert PRO PANalytical instrument equipped with a TCU 1000 temperature control unit and an Anton Paar HTK-1200 oven. The temperatures

were calibrated with phthalic acid and 4-methylbenzoic acid. Samples were prepared by melting the polymers between two Teflon plates.

General Procedure for Monomer Synthesis. A round-bottomed flask was charged with the oligoethylene glycol ditosylate and 3-bromophenol in a 1 to >2.5 molar ratio. To this was added a large excess of anhydrous K_2CO_3, DMF solvent, and a stir bar. The reaction was then left to stir overnight in a 60 °C oil bath, after which the solvent was removed via vacuum distillation. Dichloromethane was then added to the residue, and the resulting suspension was filtered to remove excess carbonate and salt byproducts. Afterwards, the solvent was removed with a rotary evaporator, and the residue was heated in a kugelrohr oven under a dynamic 5-mTorr vacuum to remove excess 3-bromophenol. The crude product was then chromatographed on silica with an eluent of hexanes/EtOAc adjusted to give an R_f for the product of 0.2−0.3. Final purification was then achieved through recrystallization and/or distillation in a bulb-to-bulb apparatus under a dynamic vacuum (<1 mTorr).

Ethylene Glycol Di(3-bromophenyl) Ether (1). The above general procedure was performed with 10.0 g (27.0 mmol) of ethylene glycol di(*p*-toluenesulfonate), 11.7 g (67.6 mmol) of 3-bromophenol, 37.3 g of K_2CO_3 (0.270 mol), and 150 mL of DMF. Ethylene glycol di(3-bromophenyl) ether (**1**) (7.19 g, 19.3 mmol, 72% yield), was then isolated as a white powder after recrystallization from methanol and distillation at 150 °C (<1 mTorr): mp 103−104 °C. ^{1}H NMR (300 MHz, $CDCl_3$): δ 7.08−7.17 (multiple resonances, 6H); 6.86 (dt, J_d = 7.8 Hz, J_t = 1.8 Hz, 2H); 4.25 (s, 4H). ^{13}C NMR (75 MHz, $CDCl_3$): δ 159.2, 130.5, 124.2, 122.8, 117.9, 113.6, 66.5. Anal. Calcd for $C_{14}H_{12}$ Br_2O_2: C, 45.19; H, 3.25; Found: C, 45.07; H, 3.03.

Diethylene Glycol Di(3-bromophenyl) Ether (2). The above general procedure was performed with 5.00 g (12.1 mmol) of diethylene glycol di(*p*-toluenesulfonate), 5.22 g (30.2 mmol) of 3-bromophenol, 16.9 g of K_2CO_3 (0.122 mol), and 60 mL of DMF. Diethylene glycol di(3-bromophenyl) ether (**2**) (3.33 g, 8.00 mmol, 66% yield) was then isolated as a white crystalline mass after recrystallization from methanol and distillation at 150 °C (<1 mTorr): mp 56 °C. ^{1}H NMR (300 MHz, $CDCl_3$): δ 7.08-7.17 (multiple resonances, 6H); 6.84 (dt, J_d = 7.5 Hz, J_t = 1.5 Hz, 2H); 4.11 (t, J = 4.2 Hz, 4H); 3.91 (t, J = 4.4 Hz, 4H). ^{13}C NMR (75 MHz, $CDCl_3$): δ 159.4, 130.5, 124.0, 122.7, 118.0, 113.6, 69.7, 67.7. Anal. Calcd for $C_{16}H_{16}$ Br_2O_3: C, 46.18; H, 3.88; Found: C, 46.22; H, 3.67.

Triethylene Glycol Di(3-bromophenyl) Ether (3). The above general procedure was performed with 10.0 g (21.8 mmol) of triethylene glycol di(*p*-toluenesulfonate), 9.65 g (54.5 mmol) of 3-bromophenol, 38.4 g of K_2CO_3 (0.278 mol), and 150 mL of DMF. Triethylene glycol di(3-bromophenyl) ether (**3**) (6.02 g, 13.1 mmol, 60% yield) was then isolated as a pale yellow oil (which solidified upon prolonged standing) after distillation at 200 °C (<1 mTorr): mp 39 °C. ^{1}H NMR (300 MHz, $CDCl_3$): δ 7.04−7.13 (multiple resonances, 6H); 6.82 (dt, J_d = 7.8 Hz, J_t = 1.8 Hz, 2H); 4.07 (t, J = 4.5 Hz, 4H); 3.82 (t, J = 4.2 Hz, 4H); 3.71 (s, 4H). ^{13}C NMR (75 MHz, $CDCl_3$): δ 159.5, 130.4, 123.8, 122.6, 117.9, 113.5, 70.7, 69.5, 67.6. Anal. Calcd for $C_{18}H_{20}$ Br_2O_4: C, 46.98; H, 4.38; Found: C, 46.73; H, 4.04.

Tetraethylene Glycol Di(3-bromophenyl) Ether (4). The above general procedure was performed with 10.0 g (19.9 mmol) of tetraethylene glycol di(*p*-toluenesulfonate), 10.4 g (60.1 mmol) of 3-bromophenol, 39.0 g of K_2CO_3 (0.282 mol), and 150 mL of DMF. Tetraethylene glycol di(3-bromophenyl) ether (**4**) (6.85 g, 13.6 mmol, 68% yield) was then isolated as a pale yellow oil after distillation at 200 °C (<1 mTorr). ^{1}H NMR (300 MHz, $CDCl_3$): δ 7.04−7.15 (multiple resonances, 6H); 6.83 (br d, J = 8.1 Hz, 2H); 4.09 (t, J = 4.5 Hz, 4H); 3.83 (t, J = 4.8 Hz, 4H); 3.66−3.74 (multiple resonances, 8H). ^{13}C NMR (75 MHz, $CDCl_3$): δ 159.8, 130.4, 124.1, 122.8, 118.4, 113.8, 71.0, 70.8, 69.7, 68.0. Anal. Calcd for $C_{20}H_{24}$ Br_2O_5: C, 47.64; H, 4.80; Found: C, 47.58; H, 4.74.

Pentaethylene Glycol Di(3-bromophenyl) Ether (5). The above general procedure was performed with 7.69 g (14.1 mmol) of pentaethylene glycol di(*p*-toluenesulfonate), 7.30 g (42.2 mmol) of 3-bromophenol, 19.7 g of K_2CO_3 (0.143 mol), and 70 mL of DMF. Pentaethylene glycol di(3-bromophenyl) ether (**5**) (5.04 g, 9.19 mmol, 65% yield) was then isolated as a pale yellow oil after distillation at 200 °C (<1 mTorr). ^{1}H NMR (300 MHz, $CDCl_3$): δ 7.05−7.15 (multiple resonances, 6H); 6.85 (dm, J_d = 7.8 Hz, 2H); 4.09 (t, J = 4.5 Hz, 4H); 3.83 (t, J = 4.5 Hz, 4H); 3.66−3.74 (multiple resonances, 8H); 3.66 (s, 4H). ^{13}C NMR (75 MHz, $CDCl_3$): δ 159.9, 130.4, 124.1, 122.8, 118.5, 113.9, 71.0, 70.8, 69.7, 68.0, (one signal not resolved). Anal. Calcd for $C_{22}H_{28}$ Br_2O_6: C, 48.20; H, 5.15; Found: C, 48.15; H, 5.18.

Hexaethylene Glycol Di(3-bromophenyl) Ether (6). The above general procedure was performed with 5.41 g (9.14 mmol) of hexaethylene glycol di(*p*-toluenesulfonate), 4.67 g (27.0 mmol) of 3-bromophenol, 12.8 g of K_2CO_3 (92.6 mmol), and 50 mL of DMF. Hexaethylene glycol di(3-bromophenyl) ether (**6**) (3.70 g, 6.26 mmol, 69% yield) was then isolated as a pale yellow oil after distillation at 200 °C (<1 mTorr). ^{1}H NMR (300 MHz, $CDCl_3$): δ 7.05−7.15 (multiple resonances, 6H); 6.84 (dm, J_d = 8.1 Hz, 2H); 4.09 (t, J = 4.5 Hz, 4H); 3.83 (t, J = 4.8 Hz, 4H); 3.64−3.74 (multiple resonances, 8H); 3.65 (s, 8H). ^{13}C NMR (75 MHz, $CDCl_3$): δ 159.7, 130.4, 124.0, 122.7, 118.3, 113.8, 70.9, 70.7, 70.6, 69.6, 67.9, (one signal not resolved). Anal. Calcd for $C_{24}H_{32}$ Br_2O_7: C, 48.67; H, 5.44; Found: C, 48.83; H, 5.59.

General Procedure for Polymer Synthesis. Exact equimolar amounts of a dibromide monomer (**1**, **2**, **3**, **4**, **5**, or **6**) and a diboronic ester monomer (**7** or **8**) were combined in a scintillation vial and dissolved in dichloromethane. This solution was transferred via pipet to a thick-walled drying ampule (100 mL for polymerizations on a 2.5 mmol scale), along with enough solvent to rinse thoroughly the vial and any pipettes used in the transfer. The ampule was charged with tri(*o*-tolyl)phosphine (0.02 mmol per mmol of dibromide) along with an efficient stir bar and fitted to a vacuum adapter with a stopcock, after which the solvent was removed *in vacuo*. Degassed 3 M aqueous K_3PO_4 (2 mL per mmol of dibromide) was then added, and the mixture was subjected to three freeze−pump−thaw cycles. Afterwards tris(dibenzylideneacetone)-dipalladium(0) (Pd_2dba_3) (0.01 mmol Pd per mmol of dibromide) dissolved in degassed dichloromethane (1 mL per mmol of dibromide) was transferred to the ampule under a nitrogen backflow. The reaction was again degassed (three freeze−pump−thaw cycles), sealed under vacuum, and placed in a 50 °C oil bath over a magnetic stirrer for 1 week. Successful polymerizations generally started out as a dark purple, which rapidly faded to colorless or pale yellow. (A dark reddish-brown was an indication of oxygen contamination, which almost always resulted in failed reactions.) At the end of this time, the ampule was broken, the aqueous phase was removed via pipet, and the crude polymer was taken up in a minimum amount of chloroform. The resulting solution (typically green, gray, or sometimes black) was then split up into centrifuge tubes and extracted with 5% aqueous NaCN until no additional bleaching occurred. (Centrifugation was often required to break the emulsions that tended to form. However, a drop of Aliquat added to the organic phase can be used to minimize their occurrence.) The organic solutions were then extracted six times with deionized water, after which the solvent was removed with a rotary evaporator. (Drying agent was NOT used, as the polymers were found to adhere to both Na_2SO_4 and $MgSO_4$.) The resulting material was then transferred to a Soxhlet thimble and extracted with water (6 h), followed by acetone (6 h), and finally either ligroin (for polymers **9**, **10**, **12**, and **14**) or toluene (for polymers **11**, **13**, and **15**) to remove cyclic oligomer impurities (6 h). After extraction into chloroform and subsequent removal of the solvent with a rotary evaporator, polymers **9**−**15** were isolated as glassy resins or opaque films.

Polymerization of 2 with 7 (Polymer 9). The above general procedure was applied using 1.0403 g (2.5000 mmol) of **2**, 0.6147 g (2.500 mmol) of **7**, 11.5 mg (0.025 mmol Pd) of $Pd_2(dba)_3$, and 15.3 mg (0.050 mmol) of tri(*o*-tolyl)phosphine. Upon workup and purification as described above, 0.672 g (2.02 mmol, 81%) of polymer **9** was isolated as a slightly yellow resin. ^{1}H NMR (300 MHz, $CDCl_3$): δ 7.60 (s, 4H); 7.32 (br t, J = 8.1 Hz, 2H); 7.18−

7.24 (multiple resonances, 4H); 6.90 (br d, $J = 7.5$ Hz, 2H); 4.21 (br, 4H); 3.95 (br, 4H). ^{13}C NMR (75 MHz, $CDCl_3$): δ 159.2, 142.1, 139.9, 129.7, 127.4, 119.8, 113.6, 113.4, 70.0, 67.6. Anal. Calcd for $C_{22}H_{20}O_3$: C, 79.49; H, 6.07; Found: C, 78.75; H, 5.80, ash, 0.19.

Attempted Polymerizations: 3 with 7, 1 with 7, and 2 with 8. The above general procedure was applied using 1.1639 g (2.5293 mmol) of **3**, 0.6219 g (2.529 mmol) of **7**, 11.5 mg (0.025 mmol Pd) of $Pd_2(dba)_3$, and 15.3 mg (0.050 mmol) of tri(*o*-tolyl)-phosphine. The resulting crude solid was subjected to Soxhlet extractions first with water, then acetone, followed by hexanes, and finally chloroform. The vast majority of the material remained insoluble. The solvent was removed from the chloroform-soluble fraction with a rotary evaporator to yield 67.4 mg (7%) of a brittle film. Analysis of this polymer by GPC showed that it was comprised of only oligomeric material ($M_n = 3220$ relative to polystyrene). As a result, further purification and analyses were not attempted. Similar results were obtained in the attempted polymerizations of **1** with **7** and **2** with **8**.

Polymerization of 4 with 7 (Polymer 10). The above general procedure was applied using 1.2676 g (2.5140 mmol) of **4**, 0.6181 g (2.514 mmol) of **7**, 11.5 mg (0.025 mmol Pd) of $Pd_2(dba)_3$, and 15.3 mg (0.050 mmol) of tri(*o*-tolyl)phosphine. Upon workup and purification as described above, 0.823 g (2.02 mmol, 74%) of polymer **10** was isolated as a slightly yellow resin. ^{1}H NMR (300 MHz, $CDCl_3$): δ 7.62 (s, 4H); 7.32 (br t, $J = 7.8$ Hz, 2H); 7.18−7.24 (multiple resonances, 4H); 6.89 (br d, $J = 8.1$ Hz, 2H); 4.18 (br t, $J = 4.2$ Hz, 4H); 3.87 (br t, $J = 4.5$ Hz, 4H); 3.73 (br, 4H); 3.71 (br, 4H). ^{13}C NMR (75 MHz, $CDCl_3$): δ 159.6, 142.4, 140.3, 129.8, 127.5, 119.9, 114.0, 113.9, 71.1, 70.9, 70.0, 68.0. Anal. Calcd for $C_{26}H_{28}O_5$: C, 74.26; H, 6.71; Found: C, 74.20; H, 6.75, ash, <0.1.

Polymerization of 4 with 8 (Polymer 11). The above general procedure was applied using 1.0902 g (2.1622 mmol) of **4**, 0.6962 g (2.162 mmol) of **8**, 11.5 mg (0.025 mmol Pd) of $Pd_2(dba)_3$, and 15.3 mg (0.050 mmol) of tri(*o*-tolyl)phosphine. Since the crude material was less soluble than the other polymers, it was first extracted into chloroform with a Soxhlet apparatus in order to bring as much as possible into solution. Further workup was then performed on this soluble fraction as described above to yield 0.580 g (1.17 mmol, 54%) of polymer **11** as an opaque white film. ^{1}H NMR (300 MHz, $CDCl_3$): δ 7.67, 7.63 (second-order AA′BB′ pattern, $J = 8.7$ Hz, 8H); 7.33 (br t, $J = 8.1$ Hz, 2H); 7.18−7.24 (multiple resonances, 4H); 6.90 (br d, $J = 7.2$ Hz, 2H); 4.18 (br t, $J = 4.5$ Hz, 4H); 3.87 (br t, $J = 4.8$ Hz, 4H); 3.73 (br, 4H); 3.71 (br, 4H). ^{13}C NMR (75 MHz, $CDCl_3$): δ 159.5, 142.3, 140.1, 139.8, 129.8, 127.5, 127.3, 119.8, 113.9, 113.7, 71.0, 70.9, 69.9, 67.9. Anal. Calcd for $C_{32}H_{32}O_5$: C, 77.40; H, 6.49; Found: C, 76.42; H, 6.29; ash, < 0.1.

Polymerization of 5 with 7 (Polymer 12). The above general procedure was applied using 0.8254 g (1.506 mmol) of **5**, 0.3703 g (1.056 mmol) of **7**, 6.9 mg (0.015 mmol Pd) of $Pd_2(dba)_3$, and 9.1 mg (0.030 mmol) of tri(*o*-tolyl)phosphine. Upon workup and purification as described above, 0.629 g (1.36 mmol, 90%) of polymer **12** was isolated as a slightly yellow resin. ^{1}H NMR (300 MHz, $CDCl_3$): δ 7.63 (s, 4H); 7.32 (br t, $J = 7.8$ Hz, 2H); 7.18−7.23 (multiple resonances, 4H); 6.90 (br d, $J = 8.1$ Hz, 2H); 4.18 (br t, $J = 4.5$ Hz, 4H); 3.87 (br t, $J = 4.5$ Hz, 4H); 3.73 (br, 4H); 3.71 (br, 4H); 3.67 (s, 4H). ^{13}C NMR (75 MHz, $CDCl_3$): δ 159.3, 142.1, 140.0, 129.7, 127.4, 119.7, 113.6, 113.5, 70.9, 70.6, 69.8, 67.6, (one signal not resolved). Anal. Calcd for $C_{28}H_{32}O_6$: C, 72.39; H, 6.94; Found: C, 71.40; H, 7.19, ash, 0.19.

Polymerization of 5 with 8 (Polymer 13). The above general procedure was applied using 0.4029 g (0.7351 mmol) of **5**, 0.2366 g (0.7351 mmol) of **8**, 3.4 mg (0.0074 mmol Pd) of $Pd_2(dba)_3$, and 4.5 mg (0.015 mmol) of tri(*o*-tolyl)phosphine. Upon workup and purification as described above, 0.324 g (0.599 mmol, 81%) of polymer **13** was isolated as a white stringy material. ^{1}H NMR (400 MHz, $CDCl_3$): δ 7.67, 7.64 (second-order AA′BB′ pattern, $J = 8.4$ Hz, 8H); 7.32 (br t, $J = 7.9$ Hz, 2H); 7.20−7.23 (multiple resonances, 4H); 6.90 (br d, $J = 8.1$ Hz, 2H); 4.17 (br t, $J = 4.6$ Hz, 4H); 3.86 (br t, $J = 4.6$ Hz, 4H); 3.72 (m, 4H); 3.68 (m, 4H); 3.66 (s, 4H). ^{13}C NMR (100 MHz, $CDCl_3$): δ 159.1, 141.9, 139.8, 139.5, 129.7, 127.4, 127.2, 119.6, 113.4, 113.2, 70.7, 70.5, 69.6, 67.3, (one signal not resolved). Anal. Calcd for $C_{34}H_{36}O_6$: C, 75.39; H, 6.71; Found: C, 74.79; H, 6.61, ash, 0.11.

Polymerization of 6 with 7 (Polymer 14). The above general procedure was applied using 1.4807 g (2.4999 mmol) of **6**, 0.6147 g (2.500 mmol) of **7**, 11.5 mg (0.025 mmol Pd) of $Pd_2(dba)_3$, and 15.3 mg (0.050 mmol) of tri(*o*-tolyl)phosphine. Upon workup and purification as described above, 0.629 g (1.36 mmol, 54%) of polymer **14** was isolated as a slightly yellow, rubbery resin. ^{1}H NMR (300 MHz, $CDCl_3$): δ 7.63 (s, 4H); 7.34 (br t, $J = 7.8$ Hz, 2H); 7.18−7.23 (multiple resonances, 4H); 6.90 (br d, $J = 7.5$ Hz, 2H); 4.18 (br t, $J = 3.9$ Hz, 4H); 3.87 (br t, $J = 3.9$ Hz, 4H); 3.65−3.74 (multiple resonances, 16H). ^{13}C NMR (75 MHz, $CDCl_3$): δ 159.3, 142.1, 140.0, 129.7, 127.4, 119.7, 113.6, 113.5, 70.9, 70.7, 70.7, 69.8, 67.6, (one signal not resolved). Anal. Calcd for $C_{30}H_{36}O_7$: C, 70.78; H, 7.13; Found: C, 68.96; H, 7.10, ash, 1.02.

Polymerization of 6 with 8 (Polymer 15). The above general procedure was applied using 1.4821 g (2.5022 mmol) of **6**, 0.8057 g (2.502 mmol) of **8**, 11.5 mg (0.025 mmol Pd) of $Pd_2(dba)_3$, and 15.3 mg (0.050 mmol) of tri(*o*-tolyl)phosphine. Upon workup and purification as described above, 0.841 g (1.44 mmol, 58%) of polymer **15** was isolated as a white stringy solid. ^{1}H NMR (300 MHz, $CDCl_3$): δ 7.69, 7.65 (second-order AA′BB′ pattern, $J = 8.4$ Hz, 8H); 7.34 (br t, $J = 7.8$ Hz, 2H); 7.19−7.25 (multiple resonances, 4H); 6.90 (br d, $J = 6.6$ Hz, 2H); 4.19 (br t, $J = 4.5$ Hz, 4H); 3.87 (br t, $J = 4.5$ Hz, 4H); 3.65−3.74 (multiple resonances, 16H). ^{13}C NMR (75 MHz, $CDCl_3$): δ 159.5, 142.3, 140.2, 139.8, 129.8, 127.6, 127.3, 119.8, 113.9, 113.8, 71.0, 70.8, 70.8, 69.9, 67.9, (one signal not resolved). Anal. Calcd for $C_{36}H_{40}O_7$: C, 73.95; H, 6.90; Found: C, 71.48; H, 6.89, ash, 0.74.

Acknowledgment. The authors gratefully acknowledge support for this work by grants from the Camille and Henry Dreyfus Foundation (Startup Award for Faculty at Undergraduate Institutions), the Donors of the Petroleum Research Fund, administered by the American Chemical Society (Type GB), the Faculty Professional Development Grant Program from the Pennsylvania State System of Higher Education Office of the Chancellor, and the West Chester University Faculty Development Committee. Light scattering and NMR instrumentation were purchased with grants from the National Science Foundation (CRIF and MRI programs, respectively). We are grateful to Mr. Adeola Ibikunle, Mr. Abidemi Orefuwa, and Prof. Andrew Goudy at Delaware State University for use of X-ray instrumentation, and their assistance in obtaining the necessary data. We would also like to thank Dr. Ulrich Klabunde for his advice on the Polarized Light Microscopy experiments, and Prof. Barbara Reisner for her assistance in interpreting the X-ray results.

References and Notes

(1) Ivory, D. M.; Miller, G. G.; Sowa, J. M.; Shacklette, L. W.; Chance, R. R.; Baughman, R. H. *J. Chem. Phys.* **1979**, *71*, 1506−1507.
(2) Schlüter, A. D. *J. Polym. Sci., Polym. Chem. Ed.* **2001**, *39*, 1533−1556 and references therein.
(3) Gin, D. L.; Conticello, V. P. *Trends Polym. Sci.* **1996**, *4*, 217−223 and references therein.
(4) Percec, V.; Hill, D. H. *ACS Symp. Ser.* **1996**, *624*, 2−56 and references therein.
(5) Schlüter, A.-D.; Wegner, G. *Acta Polym.* **1993**, *44*, 59−69 and references therein.
(6) Schlüter, A.-D.; Bo, Z. In *Handbook of Organopalladium Chemistry for Organic Synthesis*; Negishi, E., Ed.; John Wiley & Sons, Inc.: Hoboken, NJ, 2002; Vol. 1, pp 825−861 and references therein.
(7) Wu, J.; Grimsdale, A. C.; Müllen, K. *J. Mater. Chem.* **2005**, *15*, 41−52 and references therein.
(8) Bauer, R. E.; Grimsdale, A. C.; Müllen, K. *Top. Curr. Chem.* **2005**, *245*, 253−286 and references therein.

(9) Witteler, H.; Lieser, G.; Wegner, G.; Schulze, M. *Makromol. Chem. Rapid Commun.* **1993**, *14*, 471−480.
(10) Grem, G.; Leising, G. *Synth. Met.* **1993**, *55*−*57*, 4105−4110.
(11) For example, see: Fauvarque, J.-F.; Petit, M.-A.; Pflüger, F.; Jutand, A.; Chevrot, C. *Makromol. Chem. Rapid Commun.* **1983**, *4*, 455−457.
(12) Rehahn, M.; Schlüter, A.-D.; Wegner, G.; Feast, W. J. *Polymer* **1989**, *30*, 1060−1062.
(13) While parent poly(*p*-phenylene) is not planar, the measured dihedral angle is only about 20° in the solid state (Sasaki, S.; Yamamoto, T.; Kanbara, T.; Morita, A.; Yamamoto, T. *J. Polym. Sci., Polym. Phys. Ed.* **1992**, *30*, 293−297), allowing for significant conjugation between the rings. Alkyl substituents increase this angle, causing a disruption in the conjugation. For example, Grem and Leising have shown that the band gap of poly(*p*-phenylene) copolymers can be increased with the periodic incorporation of side chains onto the backbone.[10]
(14) For rigid-flexible alternating block copolymers based on poly(thiophene) derivatives, see: Harrema, J. K.; van Hutten, P. F.; Gill, R. E.; Wildeman, J.; Wieringa, R. H.; Hadziioannou, G. *Macromolecules* **1995**, *28*, 8102−8116.
(15) For nanocomposite materials formed from rigid-flexible alternating block copolymers with conjugated segments in the rigid blocks, see: Osaheni, J. A.; Jenekhe, S. A. *J. Am. Chem. Soc.* **1995**, *117*, 7389−7398.
(16) For a rigid-flexible alternating block copolymer based on a poly(*p*-phenylene ethynylene) derivative, see: Dellsperger, S.; Dötz, F.; Smith, P.; Weder, C. *Macromol. Chem. Phys.* **2000**, *201*, 192−198.
(17) For a rigid-flexible alternating block copolymer based on an oligo(*p*-phenylene vinylene) derivative, see: Zheng, M.; Ding, L.; Gürel, E.; Lahti, P. M.; Karasz, F. E. *Macromolecules* **2001**, *24*, 4124−4129.
(18) For an alternating block copolymer incorporating units of a substituted poly(*p*-phenylene), see: Bloom, P. D.; Sheares, V. V. *J. Polym. Sci., Polym. Chem. Ed.* **2001**, *39*, 3505−3512.
(19) For a recent alternating block copolymer with conjugated poly(thiophene) blocks, see: Tu, G.; Li, H.; Forster, M.; Heiderhoff, R.; Balk, L. B.; Scherf, U. *Macromolecules* **2006**, *39*, 4327−4331.
(20) Ober, C.; Lenz, R. W.; Galli, G.; Chiellini, E. *Macromolecules* **1983**, *16*, 1034−1036.
(21) For a recent example, see: Nagata, M.; Nakae, M. *J. Polym. Sci., Polym. Chem. Ed.* **2001**, *39*, 3043−3051.
(22) Schollenberger, C. S.; Dingbergs, K. *J. Elastomers Plast.* **1975**, *7*, 65−83.
(23) Wagner, Z. R.; Roenigk, T. K.; Goodson, F. E. *Macromolecules* **2001**, *34*, 5740−5743.
(24) Meurisse, P.; Noel, C.; Monnerie, L.; Fayolle, B. *Br. Polym. J.* **1981**, *13*, 55−63.
(25) Galli, G.; Chiellini, E.; Ober, C. K.; Lenz, R. W. *Makromol. Chem.* **1982**, *183*, 2693−2708.
(26) Cheng, S. Z. D.; Janimak, J. J.; Sridhar, K.; Harris, F. W. *Polymer* **1990**, *31*, 1122−1129.
(27) Ziegast, G.; Pfannemüller, B. *Polym. Bull. (Berlin)* **1981**, *4*, 467−471.
(28) Suzuki, A. *J. Organomet. Chem.* **2002**, *653*, 83−90 and references therein.
(29) Miyaura, N. *Top. Curr. Chem.* **2002**, *219*, 12−59 and references therein.
(30) Suzuki, A. In *Handbook of Organopalladium Chemistry for Organic Synthesis*; Negishi, E., Ed.; John Wiley & Sons, Inc.: Hoboken, NJ, 2002; Vol. 1, pp 249−262 and references therein.
(31) Goodson, F. E.; Wallow, T. I.; Novak, B. M. *Macromolecules* **1998**, *31*, 2047−2056.
(32) For a recent example with typical molecular weights, see: Zhou, X.-H.; Niu, Y.-H.; Huang, F.; Liu, M. S.; Jen, A. K.-Y. *Macromolecules* **2007**, *40*, 3015−3020.
(33) High molecular weights for light-emitting polymers can be achieved with a Suzuki polycondensation. For example, see: Yan, H.; Lee, P.; Armstrong, N. R.; Graham, A.; Evmenenko, G. A.; Dutta, P.; Marks, T. J. *J. Am. Chem. Soc.* **2005**, *127*, 3172−3183. However, this is an exception rather than the norm.
(34) Hyperbranched, light-emitting polymers can be formed with very high molecular weights. For example, see: Sun, M.; Li, J.; Li, B.; Fu, Y.; Bo, Z. *Macromolecules* **2005**, *38*, 2651−2658.
(35) Higher molecular weights can often be obtained with a Yamamoto, coupling polymerization. For example, see: Yang, C.; Scheiber, H.; List, E. J. W.; Jacob, J.; Müllen, K. *Macromolecules* **2006**, *39*, 5213−5221.
(36) Yamamoto, T.; Maruyama, T.; Zhou, Z.; Ito, T.; Fukuda, T.; Yoneda, Y.; Begum, F.; Ikeda, T.; Sasaki, S.; Takezoe, H.; Fukuda, A.; Kubota, K. *J. Am. Chem. Soc.* **1994**, *116*, 4832−4845.
(37) Dostál, J.; Simek, L.; Bohdanecky, M. *Polym. Bull. (Berlin)* **1998**, *41*, 123−128.
(38) For example, see: Goodson, F. E.; Hauck, S. I.; Hartwig, J. F. *J. Am. Chem. Soc.* **1999**, *121*, 7527−7539.
(39) For a recent example in which polymorphism was investigated in a similar manner, see: Ghosh, A. K.; Woo, E. M.; Sun, Y.-S.; Lee, L.-T.; Wu, M.-C. *Macromolecules* **2005**, *38*, 4780−4790.
(40) For example, see: Yandrasits, M. A.; Cheng, S. Z. D.; Zhang, A.; Cheng, J.; Wunderlich, B.; Percec, V. *Macromolecules* **1992**, *25*, 2112−2121.
(41) For a rare exception to this generality, see: Tokita, M.; Kim, K.-W.; Kang, S.; Watanabe, J. *Macromolecules* **2006**, *39*, 2021−2023.
(42) For a recent example, see: Tokita, M.; Funaoka, S.; Watanabe, J. *Macromolecules* **2004**, *37*, 9916−9921.
(43) Zheng, R.-Q.; Chen, E.-Q.; Cheng, S. Z. D.; Xie, F.; Yan, D.; He, T.; Percec, V.; Chu, P.; Ungar, G. *Macromolecules* **1999**, *32*, 6981−6988.
(44) Pardey, R.; Zhang, A.; Gabori, P. A.; Harris, F. W.; Cheng, S. Z. D.; Adduci, J.; Facinelli, J. V.; Lenz, R. W. *Macromolecules* **1992**, *25*, 5060−5068.
(45) Martínez-Gómez, A.; Pérez, E.; Bello, A. *Polymer* **2006**, *47*, 2080−2090.
(46) Teetsov, J.; Fox, M. A. *J. Mater. Chem.* **1999**, *9*, 2117−2122.
(47) Jenekhe, S. A.; Osaheni, J. A. *Science* **1994**, *265*, 765−768.
(48) For a recent example, see: Cheng, J.-A.; Chang, C.-P.; Chen, C.-H.; Lin, M.-S. *J. Polym. Res.* **2005**, *12*, 53−59.
(49) Jenekhe, S. A.; Osaheni, J. A. *Chem. Mater.* **1994**, *6*, 1906−1909.
(50) Sun, R. G.; Wang, Y. Z.; Wang, D. K.; Zheng, Q. B.; Kyllo, E. M.; Gustafson, T. L.; Wang, F.; Epstein, A. L. *Synth. Met.* **2000**, *111*−*112*, 595−602.
(51) The literature values for *p*-terphenyl and *p*-quaterphenyl are 93% and 86%, respectively.[52] However, these measurements were performed in cyclohexane. Chloroform has a pronounced 35% quenching effect on the fluorescence of terphenyl: Cohen, S. G.; Weinreb, A. *Phys. Rev.* **1954**, *93*, 1117. The quantum yields for these standards in chloroform were obtained by measuring the fluorescence and UV-absorbance in both solvents and correcting for refractive index, as described in ref 68.
(52) Berlman, I. B. *Handbook of Fluorescence Spectra of Aromatic Molecules*, 2nd ed.; Academic Press: New York, 1971.
(53) For an example of where a similar solvent correction[51] was applied, see: Musick, K. Y.; Hu, Q.-S.; Pu, L. *Macromolecules* **1998**, *31*, 2933−2942.
(54) Yang, X.; Yang, W.; Yuan, M.; Hou, Q.; Huang, J.; Zeng, X.; Cao, Y. *Synth. Met.* **2003**, *135*−*136*, 189−190.
(55) Manhart, S. A.; Adachi, A.; Sakamaki, K.; Okita, K.; Ohshita, J.; Ohno, T.; Hamaguchi, T.; Kunai, A.; Kido, J. *J. Organomet. Chem.* **1999**, *592*, 52−60.
(56) Cimrová, V.; Hlídková, H.; Vyprachticky, D.; Karastatiris, P.; Spiliopoulos, I. K.; Mikroyannidis, J. A. *J. Polym. Sci., Polym. Phys. Ed.* **2005**, *44*, 524−533.
(57) Yamamoto, T.; Sugiyama, K.; Kushida, T.; Inoue, T.; Kanbara, T. *J. Am. Chem. Soc.* **1996**, *118*, 3930−3937.
(58) Sierra, C. A.; Lahti, P. M. *Chem. Mater.* **2004**, *16*, 55−61.
(59) Kijima, M.; Matsumoto, S.; Kinoshita, I. *Synth. Met.* **2003**, *135*−*136*, 391−392.
(60) For a recent example of a similar blue shift, see: Sun, M.; Bo, Z. *J. Polym. Sci., Polym. Chem. Ed.* **2007**, *45*, 111−124.
(61) Halkyard, C. E.; Rampey, M. E.; Kloppenburg, L.; Studer-Martinez, S. L.; Bunz, U. H. F. *Macromolecules* **1998**, *31*, 8655−8659.
(62) Ding, L.; Egbe, D. A. M.; Karasz, F. E. *Macromolecules* **2004**, *37*, 6124−6131.
(63) Deng, Y.; Li, Y.; Wang, X. *Macromolecules* **2006**, *39*, 6590−6598.
(64) Neher, D. *Macromol. Rapid Commun.* **2001**, *22*, 1365−1385 and references therein.
(65) Leclerc, M. *J. Polym. Sci., Polym. Chem. Ed.* **2001**, *39*, 2867−2873 and references therein.
(66) Chen, P.; Yang, G.; Liu, T.; Li, T.; Wang, M.; Huang, W. *Polym. Int.* **2006**, *55*, 473−490 and references therein.
(67) Ouchi, M.; Inoue, Y.; Liu, Y.; Nagamune, S.; Nakamura, S.; Wada, K.; Hakushi, T. *Bull. Chem. Soc. Jpn.* **1990**, *63*, 1260−1262.
(68) Fery-Forgues, S.; Lavabre, D. *J. Chem. Educ.* **1999**, *76*, 1260−1264.

MA070796N